

## Spiraling Nested Multiwalled Carbon Nanotubes

Bo ZHANG, Faming GAO\* and Li HOU

Department of Applied Chemistry, Yanshan University, Qinhuangdao 066004, P.R. China

\*Corresponding author: E-mail: fmgao@ysu.edu.cn

(Received: 4 June 2010;

Accepted: 10 February 2011)

AJC-9603

The spiraling nested multiwalled carbon nanotubes (sn-MWCNs) with one encapsulated into the other were synthesized using solvothermal method. The growth mechanism of the sn-MWCTs was discussed. The capacitance of the nested nanotube was calculated theoretically via modeling a classical cylindrical capacitor with it.

**Key Words:** Solvothermal synthesis, Crystal growth, Nanocrystalline materials.

### INTRODUCTION

Carbon nanotubes (CNTs) are an amazingly versatile material that has key applications in transistors<sup>1</sup>, fuel cells<sup>2</sup>, TV screens<sup>3</sup>, ultra-sensitive sensors<sup>4</sup>, high-resolution AFM probes<sup>5</sup>, supercapacitors<sup>6</sup>, transparent conducting film<sup>7</sup>, drug carrier<sup>8,9</sup>, catalysts and composite material<sup>10-25</sup>. The spiraling nested multiwalled carbon nanotubes (sn-MWCNs) which are a new form of carbon nanotubes due to their special spiraling nested structure could exhibit much more excellent physical and chemical properties. Structurally, helicoidal graphite of helically shaped carbon tubules can be generated by introducing heptagons and pentagons into the predominantly hexagonal carbon framework. It is proposed that when a catalyst adheres to another one with larger size two carbon nanotubes start growing from the two catalysts respectively. Because the growing directions of them are different from each other, their growth results in a strain that impedes their growing. Relieving the strain of them in order to keep the nanotubes growing on generates spring structure accordingly. The understanding of the growth mechanism of the sn-MWCT will offer opportunity for further develop various nested nanostructures, which could lead to the manufacture of nanoelectronic devices.

In this work, we report the discovery of spiraling nested multiwalled carbon nanotubes (sn-MWCNs) with one encapsulated in the other and predict that it could be manufactured as a cylindrical nanocapacitor. We used simultaneously three catalysts to prepare carbon nanotubes with spring-like structure. It is thought that when the catalysts are of different sizes, the diameters of nanotubes based on the catalysts are different and it is possible that a nanotube with smaller diameter can nest in another nanotube with higher diameter. If the growing

directions of the two nested nanotubes are different, it would form easily spring-like coiled nanotubes. The nested nanostructures have potential applications as nanoscale cylindrical capacitors and coaxial nanocable that could serve as functional components to be integrated in micro- and nanoelectromechanical systems (MEMS, NEMS). They are also potential candidates for creating nanometer-scale devices in future nanoelectronics of the new millennium.

### EXPERIMENTAL

The spiraling nested multiwalled carbon nanotubes (sn-MWCNTs) were synthesized by a solvothermal method<sup>25</sup>. Firstly the experiment was performed in a glove compartment which was evacuated to remove the oxygen of the air and after that the N<sub>2</sub> gas was flushed into the glove compartment until it is equal to the surrounding pressure. Then 1.0 g metallic zinc powder (99 %), 1.0 g metallic nickel powder (99.99 %), 0.2 g ferrocene (98 %) and 5 mL benzene (99.5 %), 4 mL xylene (99 %), 3 mL styrene (99 %) were put into a 15 mL stainless steel autoclave. The autoclave was sealed and taken out from the glove compartment and heated in a crucible oven. The ferrocene used in this experiment decomposed and resulted in Fe particles which was smaller than Zn and Ni particles directly added into the autoclave in the form of free element. It is presumed that this ferrocene decomposition process is the key step for controlling the anisotropic growth of the sn-MWCNTs. The synthesis process was conducted at 600 °C for 24 h and cooled to room temperature naturally. The product was collected and washed with pure ethanol and distilled water several times. After that the product was dried in vacuum at 80 °C for 20 h. X-Ray powder diffraction (XRD) and

transmission electron microscopy (TEM) were used to identify the crystal structures and the nanotube sizes. The as-synthesized samples were characterized by a D/max-2500/PC X-ray diffractometer with  $\text{CuK}\alpha$  radiation ( $\lambda = 0.15418 \text{ nm}$ ), a JEM-2010 transmission electron microscope with EDS and EELS.

## RESULTS AND DISCUSSION

Transmission electron microscopy analysis shows that the as-prepared product has spring-like structure and especially there exists nested spring structure. Fig. 1 shows typical TEM images and electron diffraction pattern of the as-synthesized sn-MWCNTs. Fig. 1 (a) shows that the sn-MWCNT consists of two concentrically spiraling nested multiwalled carbon nanotubes with one encapsulated into the other. The outer carbon nanotube and inner one with approximately equal length up to  $4 \mu\text{m}$  have an average outer diameter of 300 and 120 nm, respectively. The shape of them is interesting just like the letter 'e'. Fig. 2(b) displays a bundle of helical carbon nanotubes. Several carbon nanotubes' structure in Fig. 1(b) is like the sn-MWCNT's in Fig. 1(a). In addition to the significant portion of sn-MWCNTs observed in Fig. 1(a-b). The most striking feature of the sample is the formation of spring structures of sn-MWCNTs as shown in Fig. 1(c). Fig. 1(c) displays a nested carbon nanospring. The height, average coil diameter and section diameter of the nanospring were about 860, 700 and 160 nm, respectively. The pitch of the nanospring is about 160 nm. The selected area electron diffraction (SAED) patterns in Fig. 1(d) was taken at the outer nanotube of the sn-MWCNT as indicated by arrow in Fig. 1(a). The SAED patterns from the innermost to the outer, correspond to the (002), (101), (004), (105) planes of hexagonal graphite, respectively. Fig. 1(d) shows four diffraction rings, which suggests a disordered nanocrystalline graphite structure.

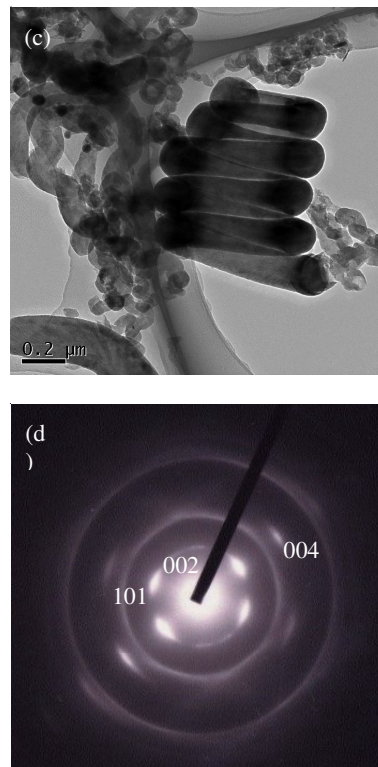
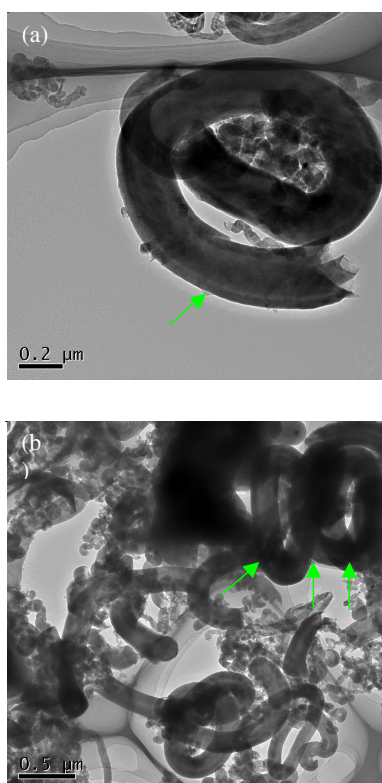


Fig. 1. (a) TEM image of a spiraling nested multiwalled carbon nanotube with one encapsulated into the other. (b) TEM image of a bundle of helical carbon nanotubes with several of them having the same structure of the sn-MWCNT in Fig. 1. (a) as indicated by arrows. (c) TEM image of a typical as-prepared nested nanotube with spring structure. (d) electron diffraction pattern recorded from the region marked in the sn-MWCNT shown in Fig. 1(a)

Fig. 2(a) shows the XRD pattern of the products before washing by dilute HCl. The two reflection peaks can be indexed to the hexagonal graphite and cubic nickel. Fig. 2(b) is the XRD pattern of the products after being washed by dilute HCl aqueous solution, which can be indexed to hexagonal graphite. The characteristic peaks of iron and zinc could not be observed, which we ascribed to the low amount of them in the sample.

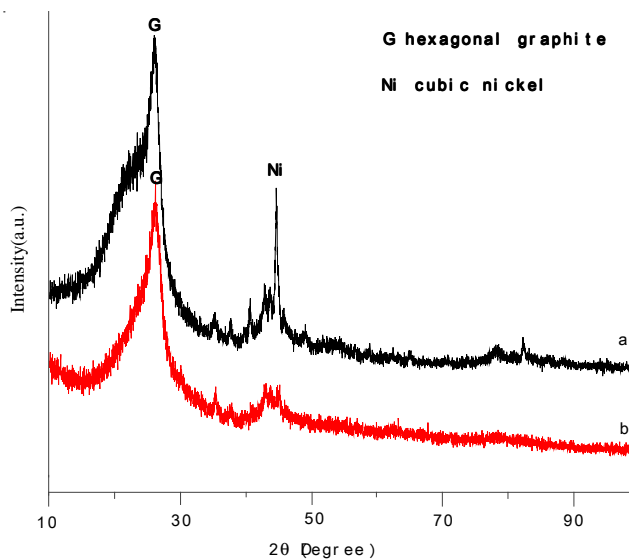


Fig. 2. X-Ray diffraction patterns of the products with different treatments: (a) not washed and (b) washed with dilute HCl aqueous solution

The growth mechanism of nested structure is formulated by us. It is thought that the use of different catalysts played a crucial role in the formation of nested structures. As shown in Fig. 3(a), the two nanotubes were grown, respectively from the tops of two catalysts of different sizes which were stuck to each other. Thus one multiwalled carbon nanotube was encapsulated into the other. Because the growing direction of them differed from each other the sustaining growth generated a strain between them which hindered their formerly straight growth. In order to overcome the strain the two nanotubes agreed to form a coil as shown in Fig. 3(b) which corresponds to the sn-MWCNT in Fig. 1(a). The lasting adsorption of carbon atoms onto the as-grown coil generated a series of coils which we called nested carbon nanosprings as shown in Fig. 3(c) which corresponds to Fig. 1(c).

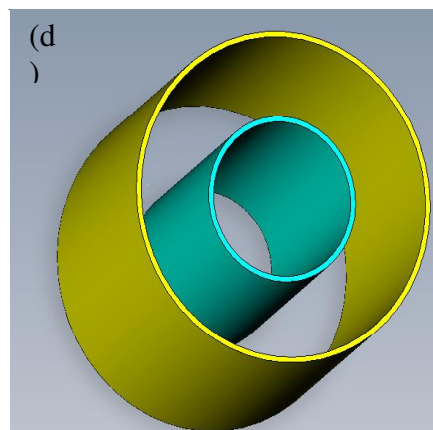
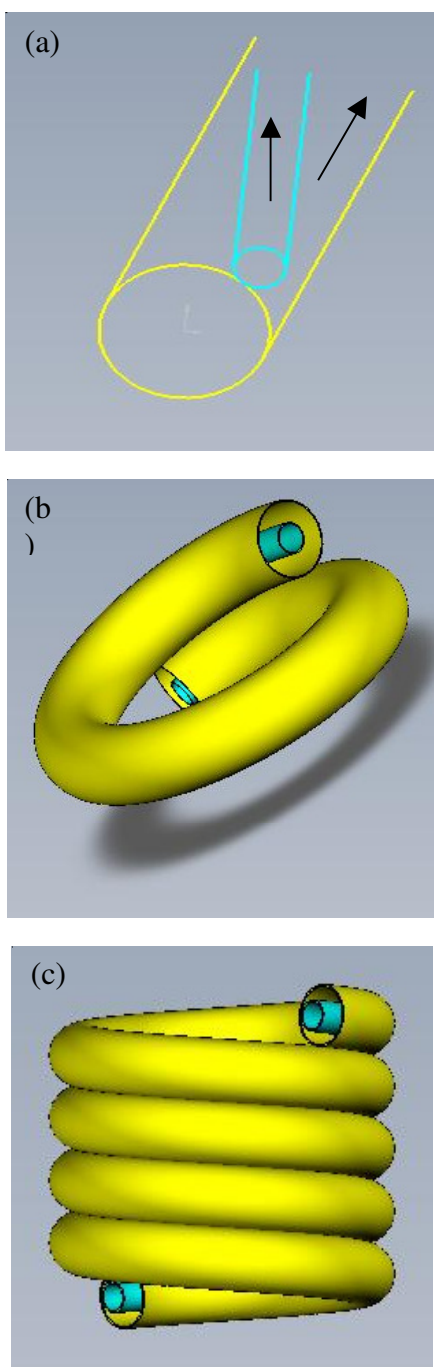


Fig. 3. (a) Schematic model showing the growth mechanism of spiraling nested nanostructures. (b) Schematic model of a one-coil sn-MWCNT corresponding to the nanotube in Fig. 1(a). (c) Schematic model of a four-coil sn-MWCNT corresponding to the nanotube in Fig. 1(c). (d) Schematic model of supposedly as-cut portion of sn-MWCNT

A further investigation reveals that the solvents and temperature of the reaction play a crucial role on the fabrication of the sn-MWCNTs. When we replaced the solvents with cyclohexane, acetone or ethanol we did not find the sn-MWCNTs. It is thought that the solvents combination of benzene, xylene and styrene due to their common hexagonal benzene ring was easy to form nest spiraling structures. It is presumed that it was worth noting that the volume ratio of benzene, xylene and styrene was 5:4:3 in the experiment. We attempted to change the ratio of three solvents, but we did not succeed in synthesizing sn-MWCNTs. All the present experiments were carried out under 600 °C which was relatively low. We performed the experiments at temperatures of 350, 400, 450, 500 and 550 °C, respectively but we did not observe sn-MWCNTs either. A detailed study is underway in present work to investigate the role of solvents and temperature in the sn-MWCNTs synthesis.

The sn-MWCNTs due to the unique nested structures could be manufactured as cylindrical nanocapacitors. In this paper we assumed to cut a length of the sn-MWCNT and supposed the as-cut portion to be two coaxial cylinders as shown in Fig. 3(d). Thus we predicted the capacitance of the as-cut sn-MWCNT with the classical calculating method of cylindrical capacitors.

Capacitance (symbol  $C$ ) is a measure of a capacitor's ability to store charge. A large capacitance means that more charge can be stored. Capacitance is measured in Faradays, symbol F. However 1F is very large, so prefixes (multipliers) are used to show the smaller values:

$\mu$  (micro) means  $10^{-6}$  (millionth), so  $1000000 \mu\text{F} = 1 \text{ F}$

$\text{n}$  (nano) means  $10^{-9}$  (thousand-millionth), so  $1000 \text{ nF} = 1 \mu\text{F}$

$\text{p}$  (pico) means  $10^{-12}$  (million-millionth), so  $1000 \text{ pF} = 1 \text{ nF}$

In vacuum, there is an isolated spherical conductor with radius  $R$  and charge  $Q$ . The potential of the charged conducting sphere is

$$V = \frac{1}{4\pi\epsilon_0} \frac{Q}{R}$$

As to the isolated spherical conductor in vacuum the capacitance is



$$C = \frac{Q}{V} = \frac{Q}{\frac{1}{4\pi\epsilon_0} \frac{Q}{R}} = 4\pi\epsilon_0 R$$

With respect to the cylindrical capacitor, as shown in Fig. 4, the calculating formula of capacitance is

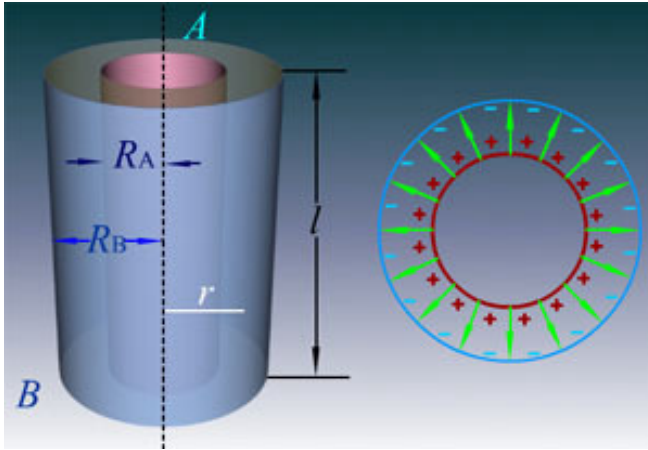


Fig. 4. Schematic model of a cylindrical capacitor

$$C = \frac{Q}{V} = \frac{2\pi\epsilon_0 l}{\ln \frac{R_B}{R_A}}$$

We established a function relationship between capacitance of as-cut sn-MWCNT and as-cut length of it. The capacitance-length function is

$$C = \frac{2\pi\epsilon_0 l}{\ln \frac{R_2}{R_1}}$$

where  $\epsilon_0$  = absolute dielectric constant of air;  $l$  = length of the as-cut sn-MWCNT;  $R_1$  and  $R_2$  = radius of the inner and outer nanotube of the as-cut sn-MWCNT, respectively. For  $\epsilon_0$  is  $8.85 \times 10^{-12} \text{ F m}^{-1}$ ;  $R_1$  and  $R_2$  are 300 and 120 nm, respectively, thus we get the capacitance-length function as follows:

$$C = \frac{2\pi \times 8.85 \times 10^{-12} \text{ F m}^{-1} \times l}{\ln \frac{300 \text{ nm}}{120 \text{ nm}}} = 3.034 \times 10^{-11} \text{ F m}^{-1} l$$

As shown in Fig. 5, it is assumed that there are four portions of the sn-MWCNT, *i.e.*,  $l$  is given four values of 10, 40, 60 and 80 nm, respectively. We calculated the capacitance of the as-cut sn-MWCNT in a discrete interval [10 nm, 80 nm]. The theoretically as-calculated capacitance values are given in Table-1.

**Conclusion**

The spiraling nested multiwalled carbon nanotubes (sn-MWCNs) with one encapsulated into the other were synthesized using solvothermal method. We have discussed the growth mechanism of the sn-MWCTs. The capacitance of the nested nanotube was calculated theoretically *via* modeling a classical cylindrical capacitor with it.

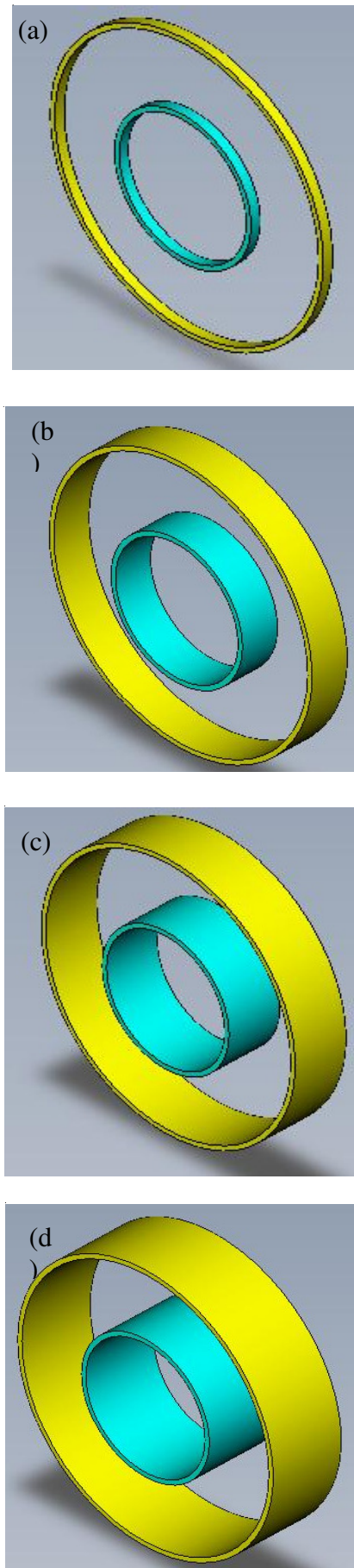


Fig. 5. (a, b, c, d) Schematic model of the four as-cut lengths of sn-MWCNT corresponding to 10, 40, 60 and 80 nm, respectively

TABLE-1  
CAPACITANCE VALUES OF THE AS-CUT  $s_n$ -MWCNT

l (m)	$1 \times 10^{-8}$	$4 \times 10^{-8}$	$6 \times 10^{-8}$	$8 \times 10^{-8}$
Capacitance (pF)	$3.304 \times 10^{-8}$	$1.322 \times 10^{-6}$	$1.982 \times 10^{-6}$	$2.643 \times 10^{-6}$

### REFERENCES

1. K. Keren, R.S. Berman, E. Buchstab, U. Sivan and E. Braun, *Science*, **302**, 1380 (2003).
2. S.S. Han, J.K. Kang, H.M. Lee, A.C.T. van Duin and W.A. Goddard, *Appl. Phys. Lett.*, **86**, 203108 (2005).
3. E. Minoux, O. Gröning, K.B.K. Teo, S.H. Dalal, L. Gangloff, J.P. Schnell, L. Hudanski, I.Y.Y. Bu, P. Vincent, P. Legagneux, G.A.J. Amaratunga and W. I. Milne, *Nano Lett.*, **5**, 2135 (2005).
4. G. Gruner, *Anal. Bioanal. Chem.*, **384**, 322 (2006).
5. J.S. Bunch, T.N. Rhodin and P.L. McEuen, *Nanotechnology*, **15**, S76 (2004).
6. K.H. An, K.K. Jeon, J.K. Heo, S.C. Lim, D.J. Bae and Y.H. Lee, *J. Electrochem. Soc.*, **149**, A1058 (2002).
7. Z. Wu, Z. Chen, X. Du, J.M. Logan, J. Sippel, M. Nikolou, K. Kamaras, J.R. Reynolds, D.B. Tanner, A.F. Hebard and A.G. Rinzler, *Science*, **305**, 1273 (2004).
8. N.W.S. Kam, Z. Liu and H. Dai, *Angew. Chem. Int. Ed.*, **44**, 1 (2005).
9. M. Ferrari, *Nat. Rev. Cancer*, **5**, 161 (2005).
10. P.G. Gollins, M.S. Arnold and P. Avouris, *Science*, **292**, 706 (2001).
11. S. Ilani, L.A.K. Donev, M. Kinderman, and P.L. McEuen, *Nat. Phys.*, **2**, 687 (2006).
12. P.R. Bandaru, C. Daraio, S. Jin and A.M. Rao, *Nat. Mater.*, **4**, 663 (2005).
13. C. Papadopoulos, A. Rikitin, A.S. Vedeneev and J.M. Xu, *Phys. Rev. Lett.*, **85**, 3476 (2000).
14. P.G. Collins and P. Avouris, *Scient. Am.*, **283**, 62 (2000).
15. M.A. Poggi, J.S. Boyles, L.A. Bottomley, A.W. McFarland, J.S. Colton, G.W. Woodruff, C.V. Nguyen, R.M. Stevens and P.T. Lillehei, *Nano Lett.*, **4**, 1009 (2004).
16. S. Tatsuura, M. Furuki, Y. Sato, I. Iwasa, M. Tian and H. Mitsu, *Adv. Mater.*, **15**, 534 (2003).
17. A.H. Barber, S.R. Cohen and H. D. Wagner, *Appl. Phys. Lett.*, **82**, 4140 (2003).
18. X. Zhao, Y. Ando, Y. Liu, M. Jinno and T. Suzuki, *Phys. Rev. Lett.*, **90**, 187401 (2003).
19. Z. Deng, E. Yenilmez, J. Leu, J.E. Hoffman, E.W.J. Straver, H. Dai and K.A. Moler, *Appl. Phys. Lett.*, **85**, 6263 (2004).
20. A. Volodin, D. Buntinx, M. Ahlskog, A. Fonseca, J.B. Nagy and C. Van Haesendonck, *Nano Lett.*, **4**, 1775 (2004).
21. K.B.K. Teo, E. Minoux, L. Hudanski, F. Peauger, J.-P. Schnell, L. Gangloff, P. Legagneux, D. Dieumegard, G.A.J. Amaratunga and W.I. Milne, *Nature*, **437**, 968 (2005).
22. H. Kajiura, H. Huang and A. Bezryadin, *Chem. Phys. Lett.*, **398**, 476 (2004).
23. C. Cui, A.A. Zakhidov, Z. Iqbal, J.N. Barisci, G.M. Spinks, G.G. Wallace, A. Mazzoldi, D. De Rossi, A.G. Rinzler, O. Jaschinski, S. Roth and M. Kertesz, *Science*, **284**, 1340 (1999).
24. D.N. McIlroy, D. Zhang, Y. Kranov and M.G. Norton, *Appl. Phys. Lett.*, **79**, 1540 (2001).
25. T. Luo, J. Liu, L. Chen, S. Zeng and Y. Qian *Carbon*, **43**, 755 (2005).